Comparison of UV and Visible Raman Spectroscopy of Bulk Metal Molybdate and Metal Vanadate Catalysts

Hanjing Tian and Israel E. Wachs*

Operando Molecular Spectroscopy and Catalysis Laboratory, Department of Chemical Engineering, Lehigh University, Bethlehem, Pennsylvania 18015

Laura E. Briand

Centro de Investigacion y Desarrollo en Ciencias Aplicadas, CONICET, Universidad Nacional de La Plata, Calle 47 No. 257 (1900), La. Plata, Buenos Aires, Argentina

Received: July 14, 2005; In Final Form: October 10, 2005

The visible (532 and 442 nm) and UV (325 nm) Raman spectra of bulk mixed metal oxides (metal molybdates and metal vanadates) were compared on the *same* spectrometer, *for the first time*, to allow examination of how varying the excitation energy from visible to UV affects the resulting Raman spectra. The quality of the Raman spectra was found to be a strong function of the absorption properties of the bulk mixed oxide. For bulk mixed metal oxides that absorb weakly in the visible and UV regions, both the visible and UV Raman spectra were of high quality and exhibit identical vibrational bands, but with slightly different relative intensities. For bulk mixed metal oxides that absorb strongly in the UV and visible regions and/or strongly in the UV and weakly in the visible regions, the visible Raman spectra are much richer in structural information and of higher resolution than the corresponding UV Raman spectra. This is a consequence of the strong UV absorption that significantly reduces the sampling volume and number of scatterers giving rise to the Raman signal. The shallower escape depth of UV Raman, however, was not sufficient to detect vibrations from the surface metal oxide species that are present on the outermost surface layer of these crystalline mixed metal oxide phases as previously suggested. It was also demonstrated that there is no sample damage by the more energetic UV excitation when very low laser powers and fast detectors are employed, thus avoiding the need of complicated fluidized bed sample arrangements sometimes used for UV Raman investigations. The current comparative Raman investigation carefully documents, *for the first time*, the advantages and disadvantages of applying different excitation energies in collecting Raman spectra of *bulk mixed metal oxide materials*.

Introduction

Visible Raman spectroscopy has proven to be a very powerful characterization technique for heterogeneous catalysts over the past three decades and has been applied to essentially all types of catalytic materials: bulk and supported metal oxides, bulk and supported metal sulfides, zeolites and molecular sieves, heteropolyoxo anions, bulk and supported metals, and clays.[1] Furthermore, visible Raman spectroscopy is also able to provide fundamental information under reaction conditions (temperature, pressure, gas, and even liquid phases), and is responsible for the current thrust in the development of the molecular structure−activity/selectivity relationships for a wide range of catalytic materials and catalytic reactions.[2] For supported metal oxide catalysts, where the metal oxides are present as a two-dimensional surface layer, the Raman vibrational spectrum directly monitors the local molecular structures and bonding of surface metal oxide complexes as well as surface reaction intermediates. Consequently, Raman can elucidate fundamental information about the nature of catalytic active surface sites and the surface reaction intermediates as well as the influence of different environmental conditions.

Occasionally, however, sample fluorescence may mask the visible Raman spectrum of catalytic materials and limit its application. Fluorescence can be caused by the presence of specific fluorescing cations (e.g., Cr^{3+}, Fe^{2+}, etc.) or some types of carbonaceous deposits.[3] Another potential limitation of visible Raman spectroscopy studies is blackbody radiation emitted by the samples at very high temperatures (T > 800 °C), which limits its application to catalytic reaction conditions below 800 °C.[4] Theoretically, laser excitation in the near-IR or UV wavelengths has the potential to avoid or minimize sample fluorescence encountered with visible excitation.[5] In the past few years, UV Raman spectroscopy has been successfully applied to the study of various zeolites and molecular sieves that typically fluorescence with visible excitation under ambient or reaction conditions.[6−9]

The recent emergence of UV Raman spectroscopy for catalyst characterization raises the question as to how UV Raman spectra compare with visible Raman spectra for the same catalytic samples under comparable collection conditions. In a previous study, the UV (244 nm) and visible Raman (514.5 nm) spectroscopic measurements of supported metal oxide systems (Al_2O_3-supported CrO_3, V_2O_5, and MoO_3 as well as TiO_2-supported MoO_3 and Re_2O_7) were examined under ambient (hydrated) and dehydrated conditions.[10] It was concluded from this comparison that (1) the intensity of UV Raman bands is generally much weaker because strong sample absorption of the UV excitation greatly reduces the sample volume and the number of scatterers, (2) the UV Raman spectrum appears to

* Address correspondence to this author. Phone: (610)-758-4274. Fax: (610)-758-6555. E-mail: iew0@lehigh.edu.

10.1021/jp053879j CCC: $30.25
Published on Web 11/16/2005

be more sensitive to the out-of-plane bending and symmetric stretching vibrations of bridging oxygen species (M−O−M), (3) the visible Raman spectrum is more sensitive to vibrations of the terminal oxygen (M═O), and (4) the higher energy of the UV excitation can readily result in surface dehydration due to laser-induced heating. This suggests that special care must be taken in the measurement of UV Raman spectra to avoid any structural transformations that may arise from the more energetic UV excitation. Such comparative Raman investigations of variable excitation energy for bulk mixed metal oxides, where the metal oxide being detected is part of the bulk network structure, have not been reported to date in the literature.

Bulk mixed metal oxides, especially metal molybdates and metal vanadates, are commercially important for many catalytic oxidation reactions (e.g., oxidation of methanol to formaldehyde, oxidation/ammoxidation of propylene/propane to acrylonitrile, oxidation of *n*-butane to maleic anhydride, etc.).[11−13] Surface metal oxides on the outermost surface of such bulk mixed metal oxides, where the catalytic active sites and surface reaction intermediates reside, have an environment that greatly differs from that of the bulk metal oxide sites. The surface cations possess fewer neighbors than the bulk cations, may be non-uniform or heterogeneous, and may directly coordinate with molecules from the gas-phase environment.[14] The investigation of the outermost surface layer of bulk mixed metal oxides is, however, very difficult by conventional spectroscopic methods because of the very small number of surface scatterers, $\sim 10^{15}$/cm^2, compared to the much larger number of bulk scatterers, $\sim 10^{19}$/cm^3. For example, for a 1 μm particle the number of surface scatterers would be $\sim 10^{23}$ and the number of bulk scatterers would be $\sim 10^{30}$ (10 million times greater for the bulk than the surface!). Consequently, very little fundamental knowledge about the composition and molecular structures of the outermost surface layer of bulk mixed metal oxides is currently available. The UV and visible Raman spectra have recently been obtained for the $Y_2O_3-ZrO_2$ mixed oxide system and the results suggest that UV Raman is much more surface sensitive than visible Raman.[15] Thus, it is important to determine if UV Raman spectroscopy is capable of providing fundamental information about the outermost surface layer of bulk mixed metal oxide catalysts.

In the present investigation, Raman spectra of a series of bulk metal molybdates and vanadates were measured, for the first time, with different laser excitation on a *combined* UV and visible Raman spectrometer system (Horiba-Jobin Yvon, LabRam-HR). The objectives of this study are (1) to determine the optimum experimental conditions for UV and visible Raman measurements, (2) to compare UV and visible Raman spectra of the same bulk mixed metal oxide catalysts with the same spectrometer, (3) compare Raman spectra of the bulk mixed metal oxide materials with the corresponding supported metal oxides previously reported, and (4) to determine if UV Raman is able to detect the outermost surface layer of bulk mixed metal oxides since previous methanol chemisorption, methanol oxidation catalytic studies, and low energy ion scattering spectroscopy (LEISS) characterization studies concluded that bulk metal molybdates and metal vanadates are surface enriched with molybdena or vanadia.[16−18]

Experimental Methods

Sample Preparation. The bulk metal molybdates ($Fe_2(MoO_4)_3$, $Cr_2(MoO_4)_3$, and $Al_2(MoO_4)_3$) were prepared by coprecipitation from $(NH_4)_6Mo_7O_{24}\cdot 4H_2O$ (Alpha Aesar Products, 99.9%) and the corresponding metal nitrate ($Fe(NO_3)_3\cdot 9H_2O$, $Cr(NO_3)_3\cdot 9H_2O$, $Al(NO_3)_3\cdot 9H_2O$, Alpha Aesar Products, 99.9%). A solution of ammonium heptamolybdate was added dropwise to the metal nitrate aqueous solutions under stirring conditions. The mixtures were maintained at 80 °C and pH 6.0 (pH 1.75 for $Fe_2(MoO_4)_3$) by adding either HNO_3 (1 M solution) or NH_4Cl (1 M solution) as needed. After aging for 3 h, the precipitates were filtered, washed with distilled water, and dried overnight at 100 °C in air. The precursors were calcined under flowing air at 400−500 °C for 4 h. The calcination temperatures depended on the specific samples since some materials crystallized more readily than others. The bulk metal vanadates ($FeVO_4$, $AlVO_4$, $CrVO_4$, and $AgVO_3$) were synthesized through an organic route from NH_4VO_3 (Alpha Aesar Products, 99.9%), the corresponding metal nitrates ($Fe(NO_3)_3\cdot 9H_2O$, $Al(NO_3)_3\cdot 9H_2O$, $Cr(NO_3)_3\cdot 9H_2O$, $AgNO_3$, Alfa Aesar or J. T. Baker, 99.9%), and citric acid ($HOC(COOH)(CH_2COOH)_2\cdot H_2O$, Alfa Aesar, 99.9%). Details of the preparations for each catalyst can be found in previous publications.[16,17]

Raman Spectroscopy. The Raman spectra of the bulk metal molybdates and vanadates were collected by a state of the art combined UV/visible Raman spectrometer system (Horiba-Jobin Yvon LabRam-HR) equipped with a confocal microscope, 2400/900 grooves/mm gratings, and a notch filter. The notch filter allows for the use of a one-stage monochromator in this system that significantly enhances the intensity of the detected photons. Two laser excitations at 442 (visible/violet) and 325 nm (UV) were generated from a He−Cd laser (Kimmon, Model: IK5751I-G, 30mW) and visible laser excitation at 532 nm (visible/green) was supplied by a Yag doubled diode pumped laser (20 mW). The scattered photons were directed and focused onto a single-stage monochromator and measured with a UV-sensitive LN_2-cooled CCD detector (Jobin Yvon CCD-3000V). The notch filter for the visible spectra had a ~ 100 cm^{-1} cutoff and the notch filter for the UV spectra had a cutoff at ~ 300 cm^{-1}. The metal molybdate and metal vanadate samples were in powder form and only 5−10 mg was usually loosely spread onto a glass slide below the confocal microscope. The laser power was typically kept below 0.5 mW (0.2 mW for UV, manufacturer measurement) to minimize any laser induced sample changes and the spectrometer resolution was greater than 2 cm^{-1}.

UV−Vis−NIR Diffuse Reflectance Spectroscopy (DRS). The DRS experiments were performed with a UV−Vis−NIR spectrophotometer system (Varian, Cary 5E). The samples were pressed into self-supporting wafers, 1 mm thick with a diameter of 1 cm, and loaded into a quartz cell with a Suprasil window. The DRS measurements were collected in the 200−600 nm regions under ambient conditions. A halon white (PTFE) reflectance standard was used as the baseline.

Results

A. Raman Spectra of Bulk $Fe_2(MoO_4)_3$ under Different Experimental Conditions. Bulk $Fe_2(MoO_4)_3$ was chosen to investigate the optimum experimental condition because of its sensitivity to UV excitation induced photochemistry.[19]

The visible (532 nm) Raman spectrum of the stationary $Fe_2(MoO_4)_3$ sample is shown in Figure 1. The new single-stage monochromator notch filter/CCD Raman system yielded a high-resolution spectrum of the stationary $Fe_2(MoO_4)_3$ sample in 1 s with 0.2 mW laser power that was essentially identical with the spectrum previously obtained with a triple-monochromator CCD Raman system (Spex Triplemate) for a spinning $Fe_2(MoO_4)_3$ sample in 900 s with 10−25 mW.[17] The $Fe_2(MoO_4)_3$ visible Raman spectrum reveals that no sample

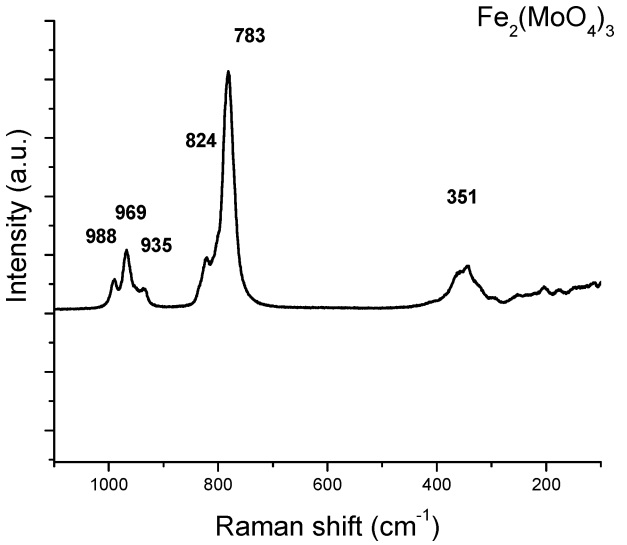

Figure 1. Visible (532 nm) Raman spectra of bulk $Fe_2(MoO_4)_3$. Experimental conditions: 2400 grooves/mm grating, notch filter/CCD, ambient, stationary, 1 s, 532 nm.

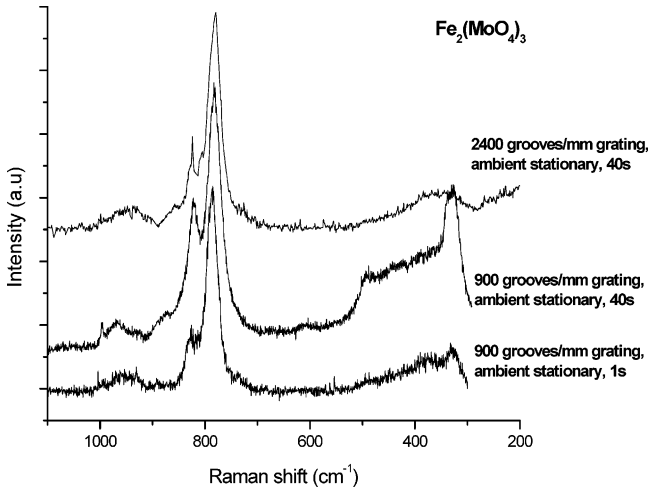

Figure 2. UV (325 nm) Raman of bulk $Fe_2(MoO_4)_3$ with different experimental conditions.

damage was done by exposing the stationary $Fe_2(MoO_4)_3$ sample to the visible laser excitation under the current experimental conditions (0.2 mW for 1 s). It also demonstrated that the new notch filter/CCD combination Raman system generates high resolution and high signal/noise ratios with very short collection times.

The UV Raman spectra of $Fe_2(MoO_4)_3$ under different experimental conditions with the same single monochromator notch filter/CCD Raman system and laser power are shown in Figure 2. The UV Raman spectrum of $Fe_2(MoO_4)_3$ with a collection time of 1 s and 900 grooves/mm grating provides an acceptable resolution and a fairly good signal/noise ratio (s/n = 15), and the signal/noise ratio improves somewhat when the collection time is increased to 40 s (s/n = 25). The UV Raman spectrum of $Fe_2(MoO_4)_3$ collected with a 2400 groove/mm grating and 40 s collection time results in much improved resolution. The UV Raman spectrum of $Fe_2(MoO_4)_3$, however, is still not comparable to the quality of the corresponding visible Raman spectrum, with a collection time of only 1 s, since the triplet of bands in the 930−990 cm^{-1} region is not resolved in the UV Raman spectrum (compare Figures 1 and 2). The UV Raman spectrum also reveals that sample damage did not occur to $Fe_2(MoO_4)_3$ from exposure to the 325 nm excitation and 0.2

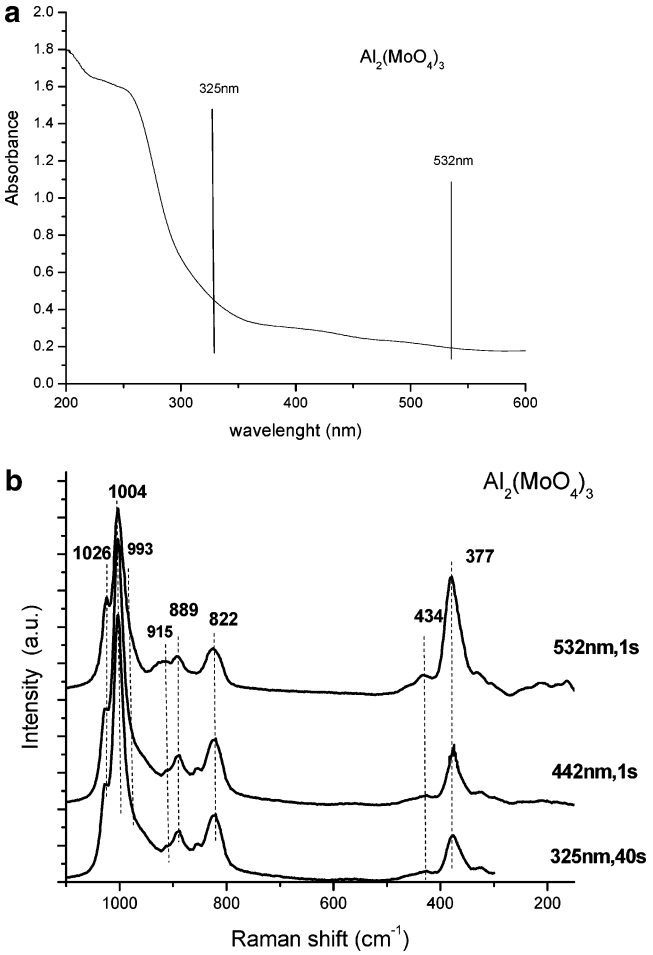

Figure 3. (a) UV−Vis diffuse reflectance spectrum of bulk $Al_2(MoO_4)_3$ and (b) Raman spectra of bulk $Al_2(MoO_4)_3$ at different wavelengths.

mW laser power. Improved quality UV Raman spectra can be obtained with longer collection times, but UV laser-induced heating and photochemical effects may affect the sample under stationary conditions. Thus, the optimum experimental conditions for the Jobin Yvon LabRam-HR Raman spectrometer were found to correspond to 2400 grooves/mm grating and collection times of 40 s for UV (325 nm) excitation and 1 s for visible (532 and 442 nm) excitation. All of the other spectra were collected under these optimum conditions.

B. Sample Possessing Weak Absorption in Both the UV and Visible Regions. Bulk $Al_2(MoO_4)_3$ contains three isolated and highly distorted MoO_4 units.[20−24] The $Al_2(MoO_4)_3$ UV−Vis DRS is presented in Figure 3a. The major UV−Vis absorption for $Al_2(MoO_4)_3$ occurs at 270 nm, which is associated with the O^{2-} to Mo^{6+} charge transfer of the isolated MoO_4 units,[22] and exhibits relatively low absorptions at the UV (325 nm) and visible (532 nm) wavelengths.

The Raman spectra of bulk $Al_2(MoO_4)_3$ obtained with the three different excitations are shown in Figure 3b. The $Al_2(MoO_4)_3$ phase is free of excess molybdenum oxide since no crystalline MoO_3 Raman bands (996, 819, and 668 cm^{-1}) are present in the UV and visible Raman spectra. The Raman bands at 1026, 1004, and ∼993 (w) cm^{-1} originate from the very short Mo═O bond of the three distinct MoO_4 units presented in $Al_2(MoO_4)_3$.[20,21] The corresponding Raman bands at 915, 889, and 822 cm^{-1} are assigned to the asymmetric stretching of the three distinct MoO_4 units. The relative intensity of the very weak 915 cm^{-1} band slightly increases with the increasing wavelength. A very small band at 857 cm^{-1} appears

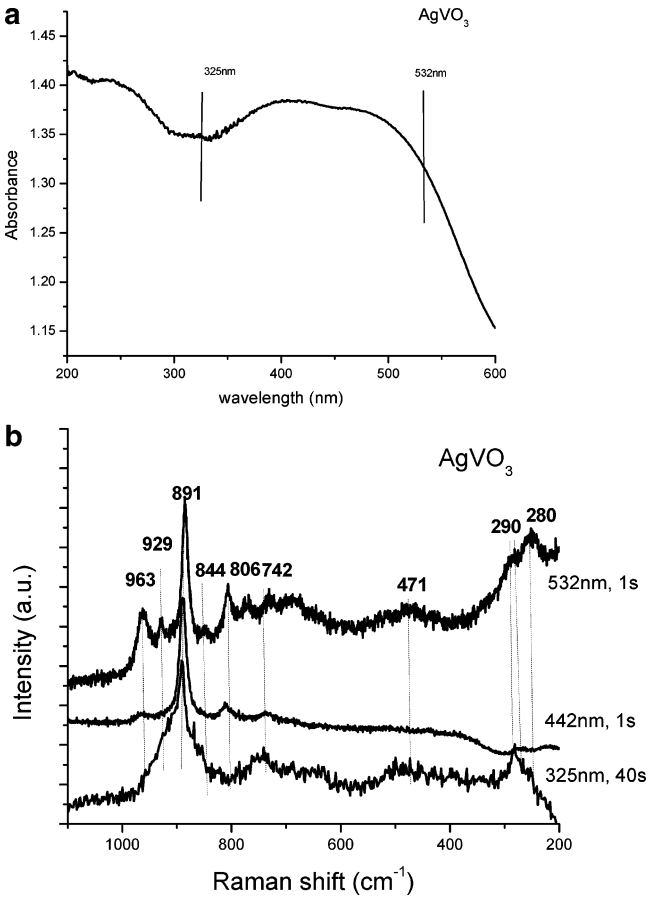

Figure 4. (a) UV−Vis diffuse reflectance spectrum of bulk $AgVO_3$ and (b) Raman spectra of bulk $AgVO_3$ at different wavelengths.

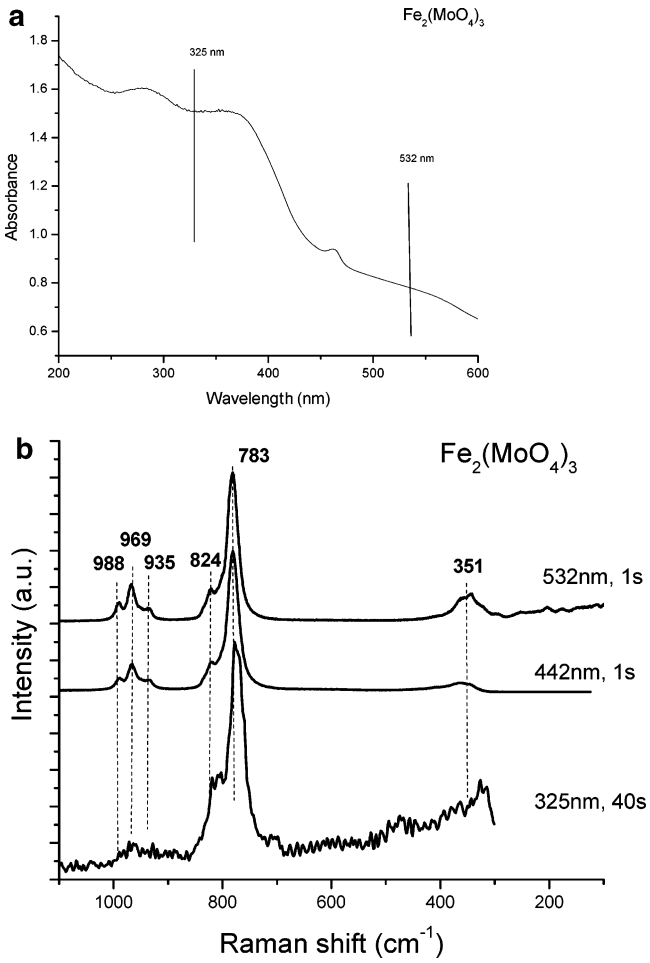

Figure 5. (a) UV−Vis diffuse reflectance spectrum of bulk $Fe_2(MoO_4)_3$ and (b) Raman spectra of bulk $Fe_2(MoO_4)_3$ at different wavelengths.

in the UV (325 nm) and visible (442 nm) Raman spectra, but is not present in the visible (532 nm) spectrum. The absence of Raman bands in 500−800 and 200−300 cm^{-1} regions is consistent with the absence of bridging Mo−O−Mo bonds in the bulk $Al_2(MoO_4)_3$ structure and confirms that the three distinct MoO_4 units are isolated. The medium intensity bands at 434 and 377 cm^{-1} are attributed to the asymmetric and symmetric bending modes of isolated MoO_4 units, respectively. The UV and visible Raman spectra of bulk $Al_2(MoO_4)_3$ exhibit identical bands, but different relative intensity. As the laser excitation decreases from visible (532 nm) to UV (325 nm) excitation, the relative intensity of the symmetric bending modes decreases. This suggests that the visible Raman is more sensitive to the symmetric bending modes than the UV Raman. Both UV and visible Raman yield high-resolution spectra of bulk $Al_2(MoO_4)_3$, which weakly absorbs in the UV and visible regions.

C. Sample Possessing Strong Absorption in Both UV and Visible Regions. Several recent papers have appeared on the bulk structures of mixed silver−vanadium oxides due to their potential application as solid electrolytes in energy storage devices.[25,26] In such Ag−V−O materials, Ag^+ cations are located between the vanadate layers and directly influence the short V═O bond. Crystalline bulk $AgVO_3$ consists of polymeric metavanadate, $(VO_3)_n^{n-}$, corresponding to single or double chains composed of polymeric VO_4 units. The UV−Vis DRS of bulk $AgVO_3$ and the corresponding Raman spectra under different laser excitations are presented in Figure 4, parts a and b, respectively. The UV−Vis DRS of $AgVO_3$ exhibits strong absorption at both the UV (325 nm) and visible (532 nm) wavelengths. In the visible Raman spectrum of $AgVO_3$, the Raman bands at 963 and 929 cm^{-1} are attributed to symmetric and asymmetric stretching of VO_4 units, respectively. The corresponding symmetric and asymmetric bending modes of the VO_4 units occur at 290 and 280 cm^{-1}, respectively. The strong band at 891 cm^{-1} may originate from either bridging V−O−Ag or O−V−O vibrations. The bridging V−O−V bond in the polymeric metavandate chains is reflected by the 742 and 471 cm^{-1} bands corresponding to the asymmetric and symmetric stretches, respectively. The weak Raman band at 806 cm^{-1} has been shown by isotopic exchange experiments to be associated with the bridging Ag−O−Ag bond.[27] The visible Raman spectrum of $AgVO_3$ indicates the high sensitivity of visible Raman to vibration of bridging M−O−M bonds. The sample is free of crystalline V_2O_5 because of the absence of its characteristic Raman bands at 994, 706, 528, and 146 cm^{-1}. The corresponding UV Raman spectrum, however, gives rise to poorly resolved bands. With the exception of the strong band at 891 cm^{-1}, all the Raman bands detected with visible excitation are overwhelmed by noise with UV excitation. Consequently, UV Raman is unable to provide additional vibrational information above that obtainable from visible Raman for bulk crystalline $AgVO_3$.

D. Samples Possessing Strong UV Absorption and Weak Visible Absorption. *1. $Fe_2(MoO_4)_3$.* Bulk iron molybdate is industrially employed as a catalyst for partial oxidation of methanol to formaldehyde under fuel-lean conditions and has been extensively researched in the past few decades.[23,28−31] Bulk $Fe_2(MoO_4)_3$ consists of three distinct, isolated MoO_4 units.[23] The UV−Vis DRS of crystalline $Fe_2(MoO_4)_3$ is shown in Figure 5a, and the absorption in the UV (325 nm) region is

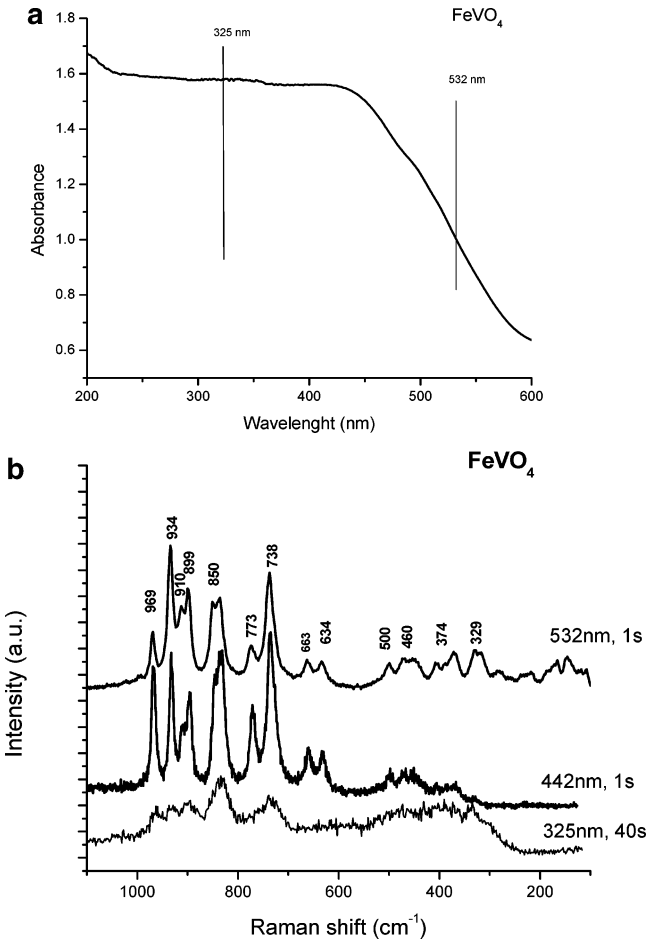

Figure 6. (a) UV−Vis diffuse reflectance spectrum of bulk $FeVO_4$ and (b) Raman spectra of bulk $FeVO_4$ at different wavelengths.

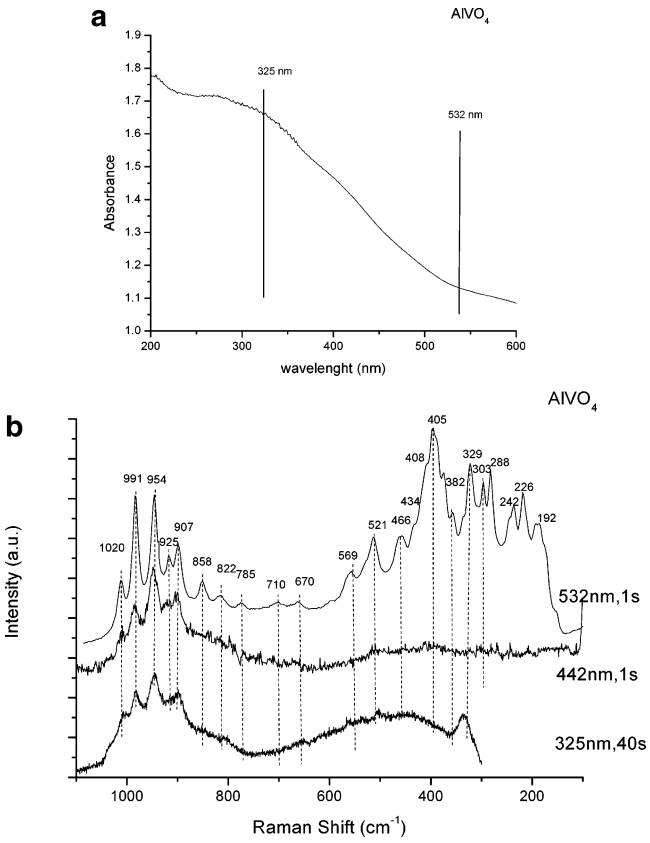

Figure 7. (a) UV−Vis diffuse reflectance spectrum of bulk $AlVO_4$ and (b) Raman spectra of bulk $AlVO_4$ at different wavelengths.

significantly stronger than absorption in the visible (532 nm) region. The broad absorption band centered at 280 nm has been attributed to the O^{2-} to Mo^{6+} charge transfer of the isolated MoO_4 sites.[30]

The Raman spectra of bulk $Fe_2(MoO_4)_3$ under different laser excitations are presented in Figure 5b. The UV and visible Raman spectra show that this sample is free of microcrystalline MoO_3 (996, 819, and 668 cm^{-1}) as well as Fe_2O_3 (676 and 221 cm^{-1}).[20] The visible Raman spectrum of bulk $Fe_2(MoO_4)_3$ exhibits a triplet of bands at 988, 969, and 935 cm^{-1} arising from the symmetric stretches of the distorted Mo═O bonds of the three distinct MoO_4 units. The vibrations at 824 and 783 cm^{-1} are the corresponding asymmetric stretching modes of the isolated MoO_4 units. The weak broad band at 351 cm^{-1} represents the MoO_4 bending modes. The lack of Raman bands in the 850−450 and 200−300 cm^{-1} regions is consistent with the absence of bridging Mo−O−Mo bonds and the exclusive presence of isolated MoO_4 units in crystalline $Fe_2(MoO_4)_3$. As the laser excitation wavelength decreases from visible (532 nm) to UV (325 nm), the relative intensity of the bands at ∼969 and 351 cm^{-1} decreases, which reveals that visible Raman is more sensitive to the symmetric stretch of terminal Mo═O bonds and bending modes than UV Raman.

2. $FeVO_4$. Crystalline $FeVO_4$ possesses a triclinic structure, belonging to the $P\bar{1}$ space group, and consists of three distinct, isolated VO_4 units.[32−34] Panels a and b of Figure 6 contain the $FeVO_4$ UV−Vis DRS and Raman spectra, respectively. Bulk $FeVO_4$ exhibits a broad UV−Vis absorption band in the 200 to 500 nm range. A detailed investigation suggests that this broad band is probably due to the overlap of two bands centered at 333 and 270 nm arising from the O^{2-} to V^{5+} charge transfer of the VO_4 units.[32] Therefore, $FeVO_4$ absorbs more strongly in the UV (325 nm) region than in the visible (532 nm) region. The visible Raman spectrum possesses a doublet of bands at 969 and 934 cm^{-1} and a third weak band estimated to occur at ∼900 cm^{-1} corresponding to the symmetric stretches of the shortest V═O bond from each of the three VO_4 units.[32] The associated asymmetric stretches appear as doublets at ∼910 and ∼899, ∼860 and ∼845, and 773 and 738 cm^{-1}, respectively. The Raman bands at ∼374 and ∼329 cm^{-1} are the associated VO_4 asymmetric and symmetric bending vibrations, respectively. The presence of bridging V−O−Fe bonds in $FeVO_4$ is reflected by asymmetric stretches at 663 and 634 cm^{-1}, symmetric stretches at 500 and 460 cm^{-1}, and weak bending modes at 200−300 cm^{-1}. The UV Raman bands are all significantly reduced in intensity and essentially masked by noise.

3. $AlVO_4$. The crystal structure of bulk $AlVO_4$ was recently determined.[35,36] $AlVO_4$ belongs to the triclinic space group and is considered to be isostructural with $FeVO_4$ with slightly more distorted isolated VO_4 units. Bulk $AlVO_4$ consists of six Al−O polyhedra that are interconnected by three independent, isolated VO_4 units. The UV−Vis DRS and Raman spectra of $AlVO_4$ under different laser excitations are shown in Figure 7, panels a and b, respectively. The UV−Vis DRS spectrum indicates a band centered at ∼280 nm and that the absorption intensity decreases from the UV (325 nm) region to the visible (532 nm) region. The highest wavenumber bands present in the visible Raman spectrum occur at 1020, 991, and 954 cm^{-1}, and correspond to the shortest V═O bonds of the three highly distorted VO_4 sites. The corresponding asymmetric stretching vibrations of the three isolated VO_4 units occur as doublets at ∼(960) and ∼(945), 925 and 907, and 858 and 822 cm^{-1}.[24] Unfortunately, the weak Raman bands expected for the most

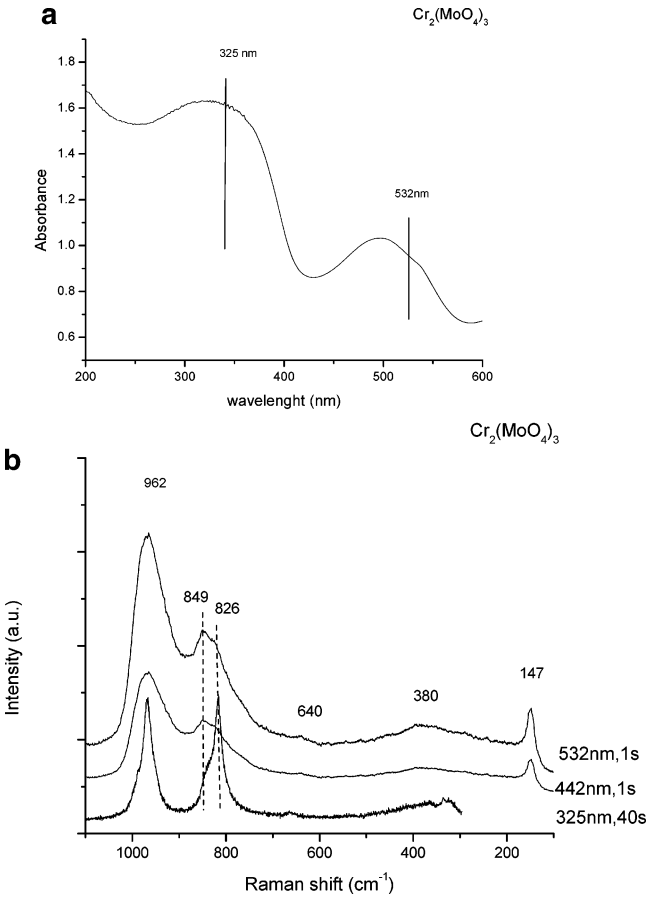

Figure 8. (a) UV−Vis diffuse reflectance spectrum of bulk $Cr_2(MoO_4)_3$ and (b) Raman spectra of bulk $Cr_2(MoO_4)_3$ at different wavelengths.

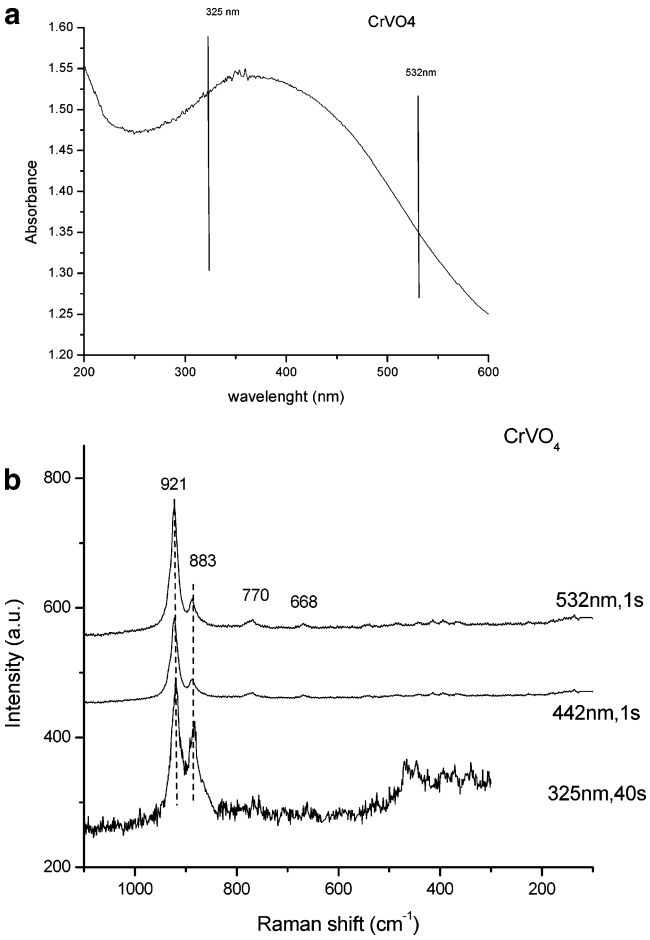

Figure 9. (a) UV−Vis diffuse reflectance spectrum of bulk $CrVO_4$ and (b) Raman spectra of bulk $CrVO_4$ at different wavelengths.

distorted VO_4 site at ∼945−960 cm^{-1} are overshadowed by the strong V═O symmetric stretch of the least distorted VO_4 site at 954 cm^{-1}. The splitting of these asymmetric stretching bands is consistent with the presence of highly distorted VO_4 sites in the bulk $AlVO_4$ structure. The associated asymmetric bending vibrations of the three isolated, distorted VO_4 sites appear at ∼434, ∼408, 405, 382, and ∼360 cm^{-1} (should be six bands, but they probably cannot all be detect because of the strong band at 405 cm^{-1}), and the corresponding symmetric stretching vibrations occur at 329, 303, and 288 cm^{-1}. In addition, vibrations originating from the bridging V−O−Al bonds are also detected in the visible Raman spectrum: asymmetric (785, 710, and 670 cm^{-1}), symmetric (569, 521, and 466 cm^{-1}), and bending (242, 226, and 192 cm^{-1}). The corresponding UV Raman spectrum of bulk $AlVO_4$ gives rise to the distorted V═O stretching vibrations of the three distinct isolated VO_4 units (1020, 991, and 954 cm^{-1}) at the same positions as in the visible Raman spectrum. However, the vibrations below 900 cm^{-1} are not detected with UV excitation due to the low intensity, high noise, and poor resolution in this region of the UV Raman spectrum of $AlVO_4$.

4. $Cr_2(MoO_4)_3$. Bulk $Cr_2(MoO_4)_3$ is reported to be isostructural with $Fe_2(MoO_4)_3$: three distinct, isolated MoO_4 units that belong to space group $P\bar{1}$ (a type).[37,38] The UV−Vis DRS and Raman spectra of $Cr_2(MoO_4)_3$ under different laser excitations are shown in Figure 8, panels a and b, respectively. The absorption at 507 nm is associated with the O^{2-} to Cr^{3+} charge transfer in the CrO_6 octahedra, while the broad peak centered at 330 nm is associated with the O^{2-} to Mo^{6+} ligand to metal charge transfer in the MoO_4 tetrahedra. Consequently, the laser excitations at 325 and 532 nm are located at almost the maximum absorptions in the UV−Vis DRS. For the visible Raman spectrum of $Cr_2(MoO_4)_3$, the broad band at 962 cm^{-1} originates from the three overlapping terminal Mo═O vibrations, and the broad band at 820−850 cm^{-1} reflects the corresponding asymmetric stretches. The related bending modes are reflected by the broad ∼380 cm^{-1} band. The sharp band at 147 cm^{-1} is assigned to the collective vibration of the $Cr_2(MoO_4)_3$ crystalline lattice. For the UV Raman spectrum of bulk $Cr_2(MoO_4)_3$, the 962 cm^{-1} band exhibits the same intensity as the 820−850 cm^{-1} band. This indicates that the MoO_4 asymmetric vibration is intensified by UV laser excitations due to the resonance Raman. In addition, the resolution of the Raman bands is improved with the UV excitation.

5. $CrVO_4$. The structure of bulk $CrVO_4$ has been extensively investigated due to its special magnetic properties.[39,40] Bulk $CrVO_4$ was reported to be isostructural with bulk $FeVO_4$.[39] Three isolated, distinct VO_4 tetrahedra are condensed with three adjacent CrO_4 chains. The UV−Vis DRS and Raman spectra of bulk $CrVO_4$, under different laser excitations, are shown in Figure 9, panels a and b, respectively. The absorption centered at 377 nm is due to the O^{2-} to V^{5+} charge transfer. Thus, the 532 and 325 nm laser excitations are located to either side of this broad absorption band. The visible Raman band at 921 cm^{-1} is assigned to overlapping symmetric stretches of three terminal V═O bonds, and the 883 cm^{-1} band is associated with the corresponding asymmetric stretching vibrations of the VO_4 units. The weak visible Raman 770 and 668 cm^{-1} bands are most likely associated with the bridging Cr−O−V bond. The UV Raman spectrum of $CrVO_4$ exhibits a lower signal/noise ratio

TABLE 1: Raman Band Positions and Assignments of Bulk Metal Molybdates and Vanadates[a]

compds	Raman shift (cm^{-1})	assignments
$Al_2(MoO_4)_3$	1026 (m), 1004 (s), ~993 (w)	terminal Mo═O bonds
	915 (w), 889 (w), 822 (w)	asymmetric stretching of MoO_4 units
	434 (w), 377 (m)	bending modes
$AgVO_3$	963 (m)	symmetric stretching of VO_4 units
	929 (w)	asymmetric stretching of VO_4 units
	891 (s)	bridging V−O−Ag or O−V−O bonds
	742 (w)	asymmetric stretch of bridging V−O−V bonds
	471 (w)	symmetric stretch of bridging V−O−V bonds
	290 (m), 280 (m)	bending modes
$Fe_2(MoO_4)_3$	988 (w), 969 (m), 935 (w)	terminal Mo═O bonds
	824 (m), 783 (s)	asymmetric stretching of MoO_4 units
	351 (w)	bending modes
$FeVO_4$	969 (m), 934 (s), (900)	terminal V═O bonds
	910 (s), 899 (s), 860 (s), 845 (s), 773 (m), 738 (s)	asymmetric stretching of VO_4 units
	663 (w), 634 (w)	bridging V−O−Fe bonds
	374 (w), 329 (w)	bending modes
$AlVO_4$	1020 (m), 991 (s), 954 (s)	terminal V═O bonds
	925 (s), 907 (m), 858 (w), 822 (w)	asymmetric stretching of VO_4 units
	785 (w), 710 (w), 670 (w)	asymmetric bridging V−O−Al bonds
	569 (w), 521 (m), 466 (m)	symmetric bridging V−O−Al bonds
	434 (m), 408 (s), 405 (s), 382 (m), 360 (m), 329 (m), 303 (m), 288 (m)	bending modes
	242 (m), 226 (m), 192 (m)	bending modes of bridging V−O−Al bonds
$Cr_2(MoO_4)_3$	962 (s)	terminal Mo═O bonds
	820−850 (s)	asymmetric stretching of MoO_4 units
	380 (w)	bending mode
$CrVO_4$	921 (s)	terminal V═O bonds
	883 (m)	asymmetric stretching of VO_4 units
	770 (w), 668 (w)	bridging Cr−O−V bonds

[a] Relative intensity based on visible (532 nm) Raman spectrum. s: strong. m: mild. w: weak.

TABLE 2: Fwhms and S/N Ratios of the Strongest Raman Band for Different Laser Excitations of Bulk Metal Molybdates and Vanadates

		fwhm		signal/noise	
compds	band position (cm^{-1})	UV Raman (325 nm)	visible Raman (532 nm)	UV Raman (325 nm)	visible Raman (532 nm)
$Al_2(MoO_4)_3$	1004	22	17	$\sim10^5$	$\sim10^5$
$AgVO_3$	891	40	12	8	16
$Fe_2(MoO_4)_3$	783	30	23	55	$\sim10^4$
$FeVO_4$	934	20	12	45	$\sim10^4$
$AlVO_4$	954	20	11	10	$\sim10^4$
$Cr_2(MoO_4)_3$	962	37	86	40	$\sim10^4$
$CrVO_4$	921	15	15	15	$\sim10^4$

than the visible spectrum, and the symmetric stretching band at 883 cm^{-1} is enhanced by UV laser excitation.

E. Summary of the Raman Spectra of Metal Molybdates and Metal Vanadates. The Raman vibrations and the assignments of the examined crystalline metal molybdates and metal vanadates are summarized in Table 1. Note that only the metal vanadate compounds gave rise to the bridging V−O−M′ Raman bands. The intensity and resolution of the UV Raman and visible Raman bands are compared in Table 2 and Table 3. The UV and visible Raman bands are comparable in intensity for class 1 compounds, but the visible Raman bands generally possess higher resolution than the corresponding UV Raman bands. An exception to this general trend is observed for $Cr_2(MoO_4)_3$ where resonance enhancement contributes to sharper UV Raman bands.

Discussion

The Raman phenomenon originates from the inelastic scattering of electromagnetic radiation by matter.[5] The theory of Raman scattering is different from that of infrared absorption, which gives rise to a complementary character, and Raman scattering is a two-photon event. For the Raman phenomenon, the polarizability of the molecule changes with respect to its vibrational motion. The interaction of the polarizability with the incoming radiation creates an induced dipole moment in the molecule, and the radiation emitted by this induced dipole moment contains the observed Raman scattering signal. In theory, the Raman signal is directly proportional to the 4th power of the excitation frequency.[1]

$$I \sim v^4 \tag{1}$$

where the term I represents the intensity of Raman scattering and v represents the frequency of the laser excitation. Thus, changing the excitation from visible wavelength (800 nm) to UV wavelength (200 nm) can increase the Raman signal intensity by as much as 256 times. However, the sample absorption also increases in going from the visible to UV excitation region as shown in the UV−Vis spectra of Figures 2a−9a. Thus, the experimentally observed changes in Raman intensity for oxides with excitation wavelength may not be as dramatic because stronger sample absorption in the UV region can greatly reduce the number of scatterers in the sampled volume (shallower escape depth).

In the current Raman investigation, the excitation frequency was varied from visible (532 nm) to UV (325 nm) that theoretically may enhance the Raman intensity by as much as 7.2 times. For the bulk metal molybdate and metal vanadates examined with 532 and 442 nm excitations no significant Raman intensity differences were observed (Raman intensity was theoretically expected to be enhanced by ~2 in going from 532 to 442 nm). However, excitation with 325 nm resulted in a much weaker Raman intensity for many of the samples. In addition, the stronger absorptions also paralleled poorer resolution and signal/noise ratios of the Raman bands as shown in Table 2. Thus, stronger sample absorption in the UV region than in the visible region of a mixed metal oxide sample significantly overwhelms the resultant UV Raman intensity relative to the

TABLE 3: Comparison of UV and Visible Raman Spectra of Bulk Metal Molybdates and Vanadates

	UV absorbance	visible absorbance	resolution		stronger vibrational modes	
			UV Raman	visible Raman	UV Raman	visible Raman
class I	low	low	very good	very good	all modes	all modes
class II	high	high	poor	vry good	none	all modes
class III	high	low	fair	very good	MO_4 asymmetric stretches	terminal M═O vibrations, MO_4 bending modes

visible Raman intensity for the examined bulk metal molybdates and metal vanadates.

The first term of the Raman polarizability tensor is given by:[1]

$$\alpha_{\alpha\beta} = \frac{1}{\hbar}\sum_{j\neq m,n}\left(\frac{\langle m|\mu_\alpha|j\rangle\langle j|\mu_\beta|n\rangle}{\omega_{jn} - \omega_o + i\Gamma_j}\right) \quad (2)$$

where $\hbar$ is Planck's constant, and the summation is over all excited electric states, j, of the molecule. The states n and m differ by a vibrational quantum of energy. The matrix element involving the operator μ_α describes the interaction of the molecule with the incident radiation, while the matrix element with the operator of μ_β represents the interaction of the molecule with the scattered radiation. The denominator expression contains several frequency-dependent terms: ω_{jn} is the angular frequency difference between the states j and n, ω_o represents the laser frequency, and the imaginary term $i\Gamma_j$ is proportional to the width of the vibration state j that is inversely proportional to its lifetime. This term is referred to as the resonance term because as the frequency difference between the transition frequency, ω_{jn}, and the laser frequency, ω_o, vanishes, the denominator of the resonance term approaches zero and its value can increase by as much as several orders of magnitude (the Raman resonance enhancement effect).

The comparison of UV and visible spectra of the bulk metal molybdates and metal vanadates is summarized in Table 3. For the samples examined in this study, the UV and visible Raman spectra exhibit the same band positions, but different relative intensity. Visible Raman is found to be more sensitive to the terminal M═O vibrations and bending modes of the bulk mixed metal oxides, and UV Raman is found to exhibit slightly enhanced asymmetric stretching vibrations of certain MO_4 units of the bulk mixed metal oxides (see Table 3 and Figures 3−9). However, no dramatic Raman resonance enhancement is observed for the UV Raman spectra of the examined bulk metal molybdates and metal vanadates.

The current findings for the comparative UV and visible Raman spectra of bulk mixed metal oxides are slightly different from the analogous Raman comparison previously reported for supported metal oxides.[10] The comparative UV and visible Raman spectra for both types of metal oxide materials exhibit identical Raman positions, but with different relative intensity and resolution. In both studies, the UV Raman intensity levels are much weaker than those of the corresponding visible Raman spectra, and visible Raman is more sensitive to the terminal M═O vibrations. However, the previous work on supported metal oxides concluded that UV Raman is more sensitive to the symmetric stretching of bridging M−O−M vibrations while this work indicates that visible Raman is more sensitive to bridging M−O−M′ vibrations of bulk mixed metal oxides. This is shown by the first reported observation of bridging V−O−Fe and V−O−Al vibrations in the visible Raman (532 nm) spectra of $FeVO_4$ and $AlVO_4$, respectively. The vibrations from bridging V−O−Al and V−O−Fe bonds are expected to occur in the 450−750 cm^{-1} range.[24] This slight difference in relative intensity of bridging vibrations between the Raman spectra of the supported metal oxides and the bulk metal oxides may be related to the fact that for supported metal oxides only the bridging M−O−M bonds of the surface metal oxide species are being detected and for bulk metal oxides the bridging M−O−M′ bonds, where M and M′ are different, of the bulk metal oxide structures are being detected. Hopefully, theoretical developments in coming years will provide additional insights on the preferential sensitivity of UV and visible Raman spectroscopy for specific vibrational modes.

Bulk metal molybdates and metal vanadates are commercially important as catalysts for the oxidation reaction of hydrocarbons. However, the current fundamental knowledge about the outermost surface layer composition and structure of such mixed metal oxide catalytic materials is essentially nonexistent. In the past few years, it was discovered with LEISS, IR of chemisorbed surface methoxy, and methanol oxidation studies that the outermost layer of bulk metal molybdates and metal vanadates consist of monolayers of surface MoOx and VOx species, respectively.[16−18] The UV and visible Raman spectra of the dehydrated surface MoOx and VOx species were previously reported[20] and exhibit their strongest Raman bands at ∼1000 and ∼1025 cm^{-1}, respectively, associated with the terminal M═O bonds. However, employing the shallower escape depth of UV Raman spectroscopy it was not possible to detect any new vibrations originating on the surface MoOx and VOx species on the outermost surfaces of bulk $AgVO_3$, $Fe_2(MoO_4)_3$, $FeVO_4$, $Cr_2(MoO_4)_3$, and $CrVO_4$. In the case of the bulk $Al_2(MoO_4)_3$ and $AlVO_4$ mixed metal oxides, however, it was not possible to monitor such bands because of the existence of strong vibrations in this region originating from the highly distorted bulk lattice MoO_4 and VO_4 units present in these structures. The similarity of bands detected with UV and visible Raman, the latter excitation possessing a significantly deeper escape depth, further confirms that both excitations are detecting the bulk metal oxide vibrations. Thus, the current UV Raman findings suggest that UV Raman is not sufficiently surface-sensitive to detect surface MoOx or VOx species on the outermost layer of bulk metal molybdates and metal vanadates.

It has recently been pointed out that UV Raman experiments may result in sample damage because of the energetic UV excitation.[7] Fluidized sample cells, where the particles are constantly moving and only have short exposure times to the energetic UV excitation, have successfully been shown to resolve this undesirable experimental artifact.[7] These earlier UV Raman studies, however, employed more energetic UV excitation (244 nm), stronger laser powers (∼100 mW), and longer collection times (∼60 min) than in the present study that tended to aggravate sample perturbation during the UV Raman experiments. In the present investigation, it was demonstrated that by employing low UV laser power (∼0.2 mW of 325 nm UV excitation at the sample) and short acquisition times, less than a minute, these experimental artifacts are not observed for the stationary bulk metal molybdate and vanadate samples employed in the current studies. Although researchers must always be

vigilant against experimental artifacts, those previously reported for UV Raman studies should not be generalized to all UV Raman investigations and systems since realistic experimental conditions exist that avoid such sample perturbations.

Conclusions

For *the first time*, comparative UV and visible Raman spectra on the *same* spectrometer were obtained for bulk mixed metal oxides that allowed for careful side-by-side comparisons. The measurements reveal that the relative quality of the resulting Raman spectra strongly depends on the absorption properties of the bulk mixed metal oxide molybdates and vanadates. For bulk mixed oxide samples that possess low absorption in the UV and visible regions (class I), very good Raman spectra are obtained with both excitations. For bulk mixed oxide samples that possess strong absorption in the UV and visible regions (class II), the resulting visible Raman spectra are richer in structural information and are of higher resolution than the corresponding UV Raman spectra. For bulk metal mixed oxides that absorb strongly in the UV region and weakly in the visible region (class III), the resulting visible Raman spectra exhibit more structural information with higher resolution than the corresponding UV Raman spectra. These Raman spectral results are a direct consequence of the strong UV absorption of many of the bulk mixed metal oxide samples, shallower escape depths, which result in weaker Raman signals and poorer resolution.

For the bulk mixed metal molybdates and metal vanadates examined in this study, significant Raman resonance enhancement was not observed and, consequently, could not compensate for the strong UV absorption by the bulk mixed metal oxide samples. Thus, visible Raman spectra of bulk mixed metal oxides are generally of higher quality and resolution than UV Raman spectra. However, only UV Raman can provide Raman spectra when occasional sample fluorescence prevents collection of visible Raman spectra.

The UV Raman spectra were found to be more sensitive to the asymmetric stretching of some of the bulk MO_4 coordinated sites. The corresponding visible Raman spectra were found to be more sensitive to bulk terminal M═O vibrations and bending modes. For the *first time*, the vibrational modes of bridging V−O−Al and V−O−Fe bonds were observed for bulk $AlVO_4$ and $FeVO_4$, respectively. The new findings for the Raman spectra of bulk mixed metal oxides are somewhat different than those previously observed for supported metal oxides. Additional comparative Raman studies between both types of metal oxide systems are needed to fully understand the origin of these differences. The shallower escape depth of UV excitation did not result in UV Raman bands from the outermost surface layer of bulk molybdates and vanadates, and both excitations only detect vibrations from the bulk structures of the mixed metal oxides. It was also demonstrated that the more energetic UV excitation did not cause any sample damage with low laser powers and rapid spectral acquisition, thus avoiding the use of fluidized bed sample systems for such UV Raman investigations.

Acknowledgment. This research was supported by the Department of Energy (DOE), division of Basic Energy Sciences (93-ER14350). Funds for the acquisition of the new state of the art spectrometer system were provided by DOE-BES (93-ER14350), NSF (CTS-0213377), Lehigh University, and Horiba-Jobin Yvon, Inc. The authors also acknowledge the NSF-CONICET (US−Argentina) collaboration program (Res. NO. 0060).

References and Notes

(1) Wachs, I. E. In *Handbook of Raman Spectroscopy*; Lewis I. E., Edwards H. G., Eds.; Marcel Dekker: New York, 2001.
(2) Banares, M. A.; Wachs. I. E. *J. Raman Spectrosc*. **2002**, *33*, 333.
(3) Dutta, P. K.; Zaykoski, R. E. *Zeolites* **1988**, *8*, 179.
(4) Zouboulis, E.; Renusch, D.; Grimsditch, H. *Appl. Phys. Lett*. **1998**, *72*, 5.
(5) Nafie, L. A. In *Handbook of Raman Spectroscopy*; Lewis I. E., Edwards H. G., Eds.; Marcel-Dekker: New York, 2001.
(6) Li, M.; Feng, Z.; Xiong, G.; Ying, P.; Li, C. *J. Phys. Chem*. **2001**, *105*, 8107.
(7) Chua, Y. T.; Stair, P. C. *J. Catal*. **2000**, *196*, 66.
(8) Li, C.; Guang, X.; Qin, X. *Angew. Chem., Int. Ed*. **1999**, *38*, 2220.
(9) Li, C.; Guang, X.; Jianke, L.; Pingliang, Y. *J. Phys. Chem. B* **2001**, *105*, 2993.
(10) Chua, Y. T.; Stair, P. C.; Wachs, I. E. *J. Phys. Chem. B* **2001**, *105*, 8600.
(11) Thorsteinson, E. M.; Wilson, T. P.; Young, F. G.; Kasai, P. H. *J. Catal.* **1978**, *52*, 116.
(12) Madeira, L. M.; Portela, M. F. *Catal. Rev. Sci. Eng.* **2002**, *44*, 247.
(13) Martin, R. M.; Portela, M. F.; Madeira, L. M.; Freire, F.; Oliveira. M. *Appl. Catal. A* **1995**, *127*, 201.
(14) Somorjai, G. A. *Introduction to Surface Chemistry and Catalysis*; Wiley-Interscience: New York, 1994; p 271.
(15) Li, C.; Meijun, L. *J. Raman Spectrosc.* **2002**, *33*, 301.
(16) Briand, L. E.; Hirt, A. M.; Wachs, I. E. *J. Catal*. **2001**, *202*, 268. Briand, L. E.; Jehng, J.-M.; Cornaglia, L.; Hirt, A. M.; Wachs, I. E. *Catal. Today* **2003**, *78*, 257.
(17) Burcham, L. J.; Briand, L. E.; Wachs, I. E. *Langmuir* **2001**, *17*, 6175.
(18) Gruenert, W.; Briand, L. E.; Tkachenko, O. P.; Tolkatchev, N. N.; Wachs, I. E. Presented at the 228th National Meeting of the American Chemical Society, Philadelphia, PA, August 22−26, 2004; Division of Colloids and Surface Chemistry, paper no. 58.
(19) Tian, H.; Briand, L.; Li, C.; Wachs, I. E. *Proc. 18th North Am. Catal. Soc. Meeting, Cancun, Mexico* **2003**, 220.
(20) Jehng, J.-M.; Wachs, I. E.; Clark, F. T.; Springman, M. C. *J. Mol. Catal.* **1993**, *81*, 63.
(21) Hu, H.; Wachs, I. E. *J. Phys. Chem*. **1995**, *99*, 10911.
(22) Forzatti, P.; Mari, C. M.; Villa, P. *Mater. Res. Bull*. **1987**, *22*, 1593.
(23) Hardcastle, F. D.; Wachs, I. E. *J. Raman. Spectrosc*. **1990**, *21*, 683
(24) Hardcastle, F. D.; Wachs, I. E. *J. Phys. Chem.* **1991**, *95*, 10763.
(25) Lewandowska, R.; Krasowski, K.; Bacewicz, R.; Garbaczyk, J. E. *Solid State Ionics* **1999**, *119*, 229.
(26) Garbarczyk, J. E.; Machowski, P.; Wasiucionek M.; Tykarski, L.; Bacewicz, R.; Aleksiejuk, A. *Solid State Ionics* **2000**, *136/137*, 1077.
(27) Wang, C. B.; Deo, D.; Wachs. I. E. *J. Phys. Chem.* **1999**, *103*, 5645.
(28) Ponceblanc, H.; Millet, J. M.; Herrmann, J. M. *J. Catal.* **1993**, *142*, 373.
(29) Hill, C. G.; Wilson, J. H. *J. Mol. Catal.* **1990**, *63*, 65.
(30) Kovats, W. D.; Hill, C. G. *Appl. Spectrosc.* **1986**, *40*, 1215.
(31) Mestl, G. *J. Raman. Spectrosc*. **2002**, *33*, 333.
(32) Kurzawa, M.; Tomaszewicz, E. *Spectrochim. Acta Part A* **1999**, *55*, 2889.
(33) Oka, Y.; Yao, T.; Yamamoto, N. *J. Solid State Chem*. **1996**, *123*, 54.
(34) Vuk, A. S.; Orel, B.; Drazic, G.; Colomban, P. *Monatsh. Chem.* **2002**, *133*, 889.
(35) Coelho, A. A. *J. Appl. Crystallogr*. **2000**, *33*, 899.
(36) Arisi, E.; Palomares, S. A.; Leccabue, F.; et al. *J. Mater. Sci*. **2004**, *39*, 2107.
(37) Forzatti, P.; Mari, C. M.; Villa, P. *Mater. Res. Bull*. **1987**, *22*, 1593.
(38) Harrison, W. T.; Cheetham, A, K.; Faber, J. *J. Solid State Chem.* **1988**, *76* (2), 328.
(39) Koo, H, J.; Whangbo, M. H.; Lee, K. S. *Inorg. Chem*. **2003**, *42*, 5932.
(40) Frazer, B. C.; Brown, P. J. *Phys. Rev. B* **1962**, *125*, 1283.